Original Article

Estimation of soil erosion and sediment yield in Wadi El Hachem watershed (Algeria) using the RUSLE-SDR approach

SAOUD Mohammed[1,2,3*] https://orcid.org/0000-0002-0983-4664; e-mail: saoud187@gmail.com

MEDDI Mohamed[2] https://orcid.org/0000-0002-9772-7366; e-mail: m.meddi@ensh.dz

Corresponding author

1 Higher National School of Agronomy (ENSA), El Harrach 16004, Algiers, Algeria

2 Génie de l'Eau et Environnement Laboratory, Higher National School of Hydraulics (ENSH), P.O. box 31 Blida 09000, Algeria

3 National Institute for Forest Research (INRF), P.O. box 37 Cheraga 16014, Algiers, Algeria

Abstract: One of the most common types of soil degradation is water erosion. It reduces soil quality at the erosion site and may cause sedimentation issues at the deposition site. This phenomenon is estimated using a variety of models. The Revised Universal Soil Loss Equation (RUSLE) model is the most often used, due to its consistence and low data requirement. It is useful for estimating annual soil loss at the watershed scale. To investigate the relationship between soil erosion and sediment deposition, the combined RUSLE and Sediment Delivery Ratio (SDR) models are used. The Wadi El Hachem watershed is a coastal and mountainous Mediterranean basin with rugged topography and high degree of climatic aggressiveness. Both of these characteristics can have an immediate effect on soil erosion and sediment yield. This research includes estimating the Average Annual Soil Loss (A) and Sediment Yield (SY) in the Wadi El Hachem watershed, mapping different RUSLE factors as well as A and SY, and studying the influence of rainfall erosivity (R) on A and SY in dry and rainy years. The A results vary from 0 to 410 t·ha⁻¹·yr⁻¹ with an annual average of 52 t·ha⁻¹·yr⁻¹. The Renfro's SDR model was selected as the best model for estimating SY, with standard error, standard deviation, coefficient of variation, and Nash–Sutcliffe efficiency (NSE) values of 0.38%, 0.02, 0.07%, and 1.00, respectively. The average SY throughout the whole watershed is around 27 t·ha⁻¹·yr⁻¹. The SY map for the entire Wadi El Hachem watershed revealed that sediment production zones are mainly concentrated in the Northeast of the basin, at the basin's outlet, and in the tributaries of the dam. The simulation results of soil loss and sediment yield in dry and rainy years revealed that R is one of the main factors affecting soil erosion and sediment deposition in the Wadi El Hachem watershed. The mean difference in R factor between dry year and rainy year is 671 MJ·mm·ha⁻¹·h⁻¹·yr⁻¹. As a result of this fluctuation, the soil loss and sediment yield have increased by 15 and 8 t·ha⁻¹·yr⁻¹, respectively. The results of this research can be used to provide scientific and technical support for conservation and management strategies of the Wadi El Hachem watershed.

Keywords: RUSLE; Sediment delivery ratio; Soil loss; Sediment yield; Wadi El Hachem; Algeria

1 Introduction

Water erosion is one of the most serious forms of

soil degradation (Ferreira et al. 2022). It is defined as the rapid loss of topsoil from the land surface caused by water (FAO and ITPS 2015). Water erosion is a very common phenomenon that decreases soil quality in erosion area (on-site effect) and can lead to sedimentation problems in deposition area (off-site effect) (Osman 2014). According to FAO and ITPS (2015), the amount of eroded soil worldwide is estimated to be between 20 and 30 Gt per year, corresponding to a loss of 0.90 to 0.95 mm of soil from the land surface. As a result, an adequate assessment of soil loss is required to determine the degree and severity of soil erosion using an appropriate soil loss model (Alewell et al. 2019).

Water erosion is estimated using a variety of models. These models are classified into three categories: empirical, semi-empirical and physical models (Merritt et al. 2003). Revised Universal Soil Loss Equation (RUSLE), an empirical model, is the most commonly used due to its consistence and low data requirement (Bhandari et al. 2015; Rajbanshi and Bhattacharya 2020). This model is suitable for assessing annual soil loss at the watershed scale in a variety of landscapes and under a variety of land cover conditions (Zini et al. 2015; Kumar 2020). This model has been widely applied to estimate water erosion in Algeria (Benchettouh et al. 2017; Meghraoui et al. 2017; Djoukbala et al. 2018; Toubal et al. 2018; Sahli et al. 2019) and in several countries throughout the world (Wall et al. 2002; Fu et al. 2006; López-Vicente et al. 2008; Farhan and Nawaiseh 2015; Nasir and Selvakumar 2018; Mukanov et al. 2019; Phinzi and Ngetar 2019; Schmidt et al. 2019; Chafai et al. 2020; Jaafari and Benabdelhadi 2020).

It is crucial to investigate the relationship between soil erosion and sediment deposition in water erosion studies (Jain and Das 2009; Hui et al. 2010). However, the RUSLE model assesses soil erosion only, and does not take into account sediment yield. This feature is considered to be one of the model's limitations (Phinzi and Ngetar 2019). This constraint can be overcome by including the sediment delivery ratio (SDR) into the RUSLE model, resulting in the RUSLE-SDR combination. The SDR for a specific watershed is the fraction of the eroded soil that reaches a continuous stream system. It is influenced by a variety of geomorphological, hydrological, and environmental watershed factors (Fu et al. 2006). SY in a drainage basin is estimated using this combination by multiplying soil loss and

SDR (Bhattacharya and Das Chatterjee 2021). The combined RUSLE-SDR model has been widely applied in recent years for assessing both A and SY at the watershed scale (Saygın et al. 2014; Magesh and Chandrasekar 2016; Colman et al. 2018; Ebrahimzadeh et al. 2018; Thomas et al. 2018; Singh et al. 2019; Rajbanshi and Bhattacharya 2020; Bhattacharya and Das Chatterjee 2021; Tsegaye and Bharti 2021; Ben Cheikha et al. 2021; Menasria et al. 2021; Ouadja et al. 2022).

This model is applied in a coastal and mountainous Mediterranean basin, such as the Wadi El Hachem watershed in Northern Algeria. This region is characterized by a rugged topography and a high degree of climatic aggressiveness, both of which can have a direct impact on the triggering of water erosion and the production of sediments.

The objectives of this study are (i) estimating the average annual soil loss and sediment yield in the watershed of Wadi El Hachem, (ii) mapping different RUSLE factors as well as the soil loss and sediment yield, and (iii) analyzing and anticipating the impact of rainfall erosivity on soil loss and sediment yield in dry and rainy year.

2 Study Area

The Wadi El Hachem watershed is a coastal basin situated in the Northern part of Algeria, in the Wilaya of Tipaza. It is located between 36.4125° and 36.6139°N, and between 2.1286° and 2.3625°E (Fig. 1). It covers an area of 220 km². The Wadi El Hachem watershed is part of the Tellian Atlas bordered by the Mediterranean. In fact, mountains cover two-thirds of the watershed area. They are represented by the Chenoua massif in the north, and the BouMaad mountain in the south and west of the watershed. The average altitude of the basin is around 400 m. The slope varies between 0 and 124% with an average value of 30% (Fig. 2). The study region has a Mediterranean climate, with a mild winter and a hot summer. The average annual rainfall and temperature values are 532 mm and 18.5°C, respectively. The geological formations encountered in the study area are predominantly sedimentary rocks with a percentage of 91%. The remainder is represented by eruptive rocks (9%). The main sedimentary rocks encountered are shales and limestones, clayey marls, blue marls, calcareous and schistose marls, gravels
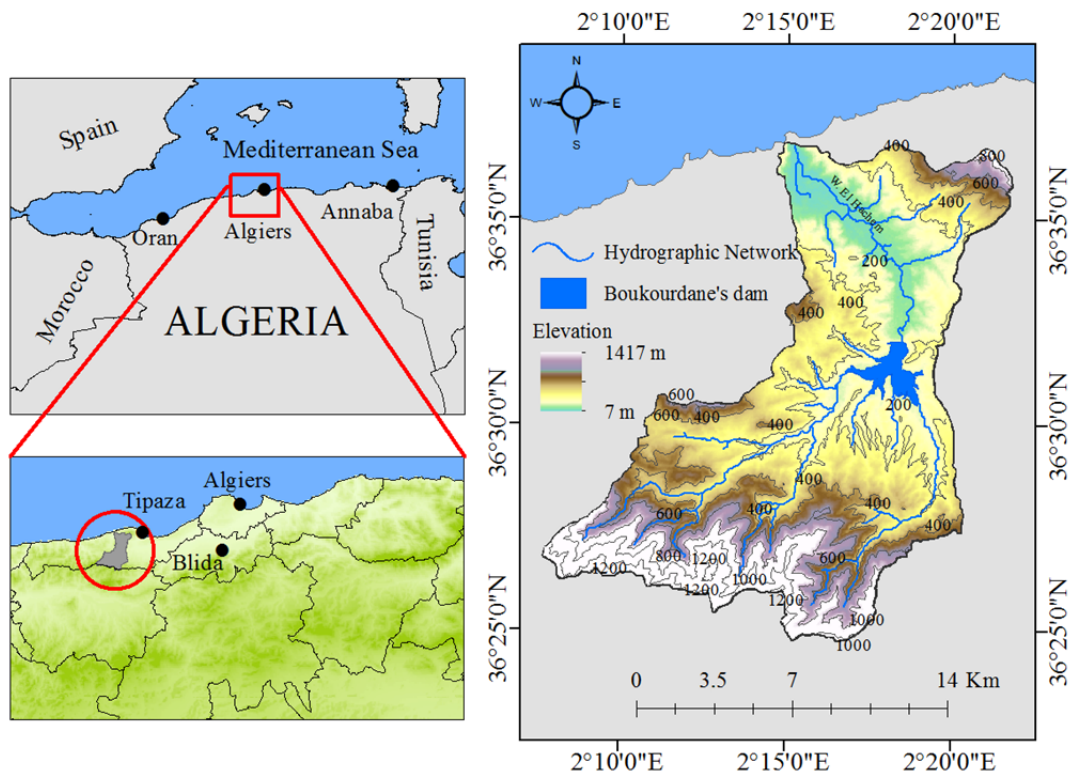
Fig. 1 Localization of the Wadi El Hachem watershed.
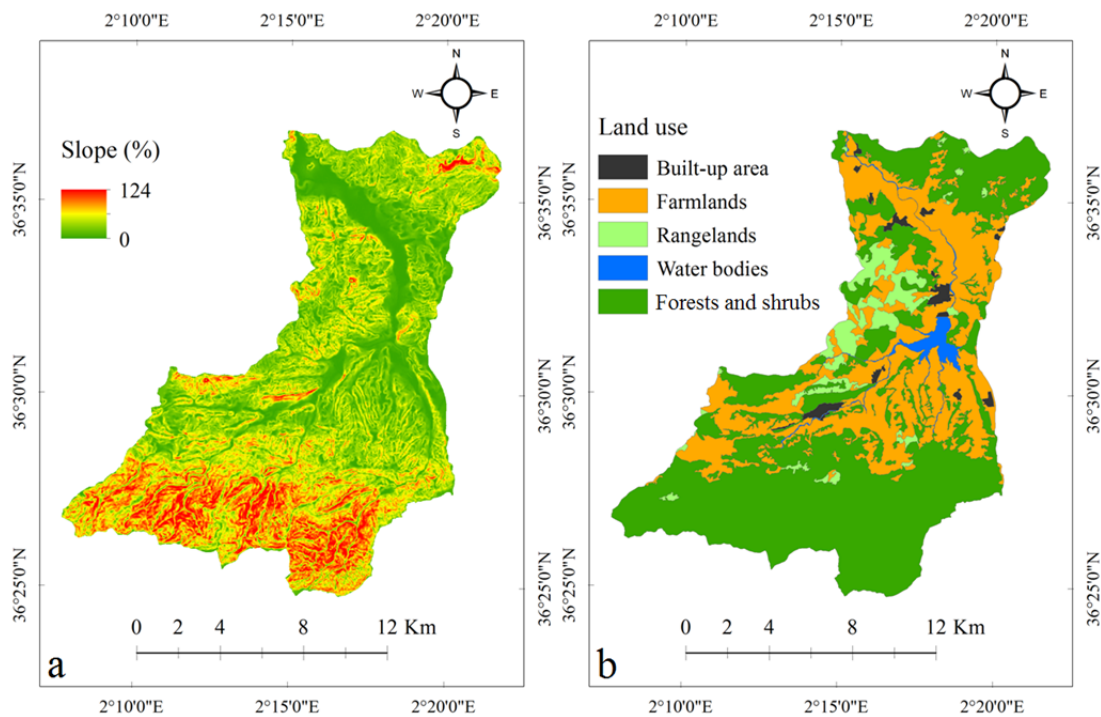
Fig. 2 Slope (a) and land use (b) maps of the Wadi El Hachem watershed.

and alluvial deposits (Saoud and Meddi 2022). The land use of the watershed is mainly represented by forest lands (59%), which are mostly found in mountains and hills. Agricultural lands cover 32% of the watershed area. They are mainly found in the north along the Wadi El Hachem valley, and in the foothills at the central and western parts of the watershed. Rangelands, water bodies and built-up

areas account for less than 10% of the total area (Fig. 2). The Boukourdane dam, which is part of the Wadi El Hachem watershed (Fig. 1), was built in 1993 with a useful capacity of 97 hm³ and allows for the regulation of 50 hm³. It is intended for drinking water supply and irrigation of the valley of Wadi El Hachem and the coastal plain of Tipaza.

3 Materials and Methods

In order to accomplish the objectives of this study using the combined RUSLE-SDR model, the research methodology involves two types: (i) the estimation of soil loss (A) using the RUSLE model, and (ii) the calculation of sediment yield (SY) using the sediment delivery ratio (SDR) model. This methodology is presented in the form of a flowchart (Fig. 3).

3.1 Soil loss estimation

In this study, the average annual soil loss of the Wadi El Hachem watershed is estimated by RUSLE model, as shown by (Eq. 1):

$$A = R \times K \times LS \times C \times P \qquad (1)$$

where A is the average annual soil loss (t·ha⁻¹·yr⁻¹), R is the rainfall-runoff factor (MJ·mm·ha⁻¹·h⁻¹·yr⁻¹), K is the soil erodibility factor (t·h·MJ⁻¹·mm⁻¹), LS is slope length and steepness factor, C is the cover-management factor, and P is the support practice factor.

The R factor is the rainfall-runoff erosivity index used to predict water erosion. Due to the lack of data required to calculate this factor by using the original formula, Meddi et al. (2016) developed an alternative equation (Eq. 2) adapted to Algerian conditions, which was used in our study:

$$R = 0.47 \, MFI^{0.49} \times X^{0.12} \times Z^{-0.05} \times Pjmax^{0.99} \quad (2)$$

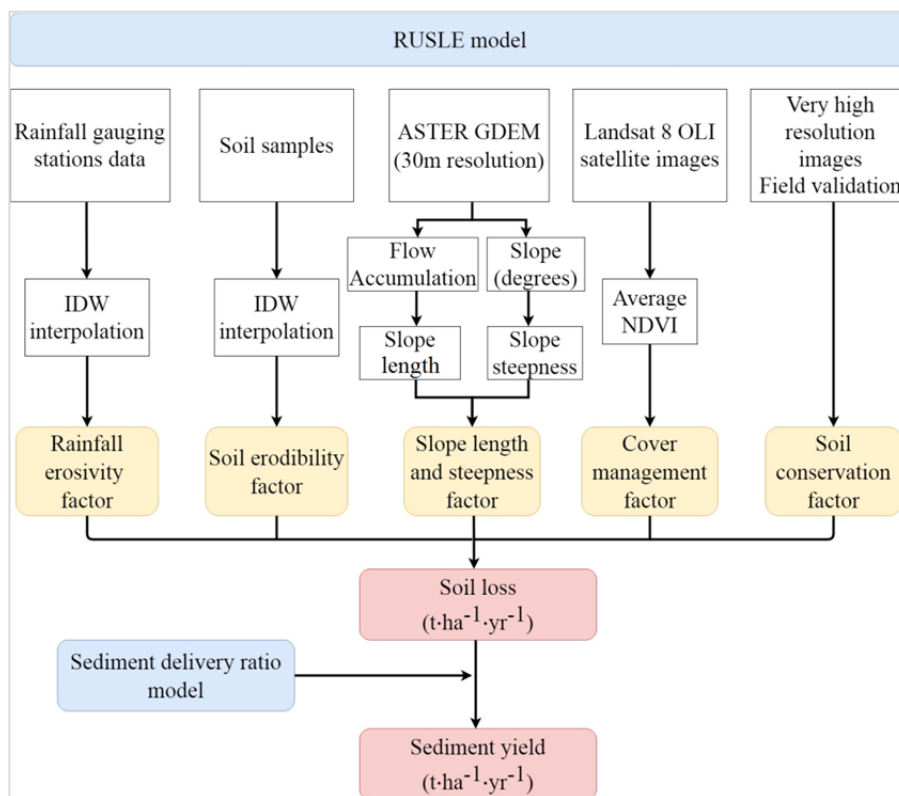
Fig. 3 Presentation of the methodology used.

where MFI is the Modified Fournier Index (mm), X is the longitude (km), Z is the altitude (m), and Pjmax is the maximal daily rainfall (mm).

We used six rainfall gauging stations located throughout the watershed (Table 1) which have the data required to calculate the R factor using Eq. 2. The number of years of climatic data recorded varies between 22 to 46, with data collected from 1967 to 2014. An annual average value of the R factor was computed for each rainfall station. As a result, the R factor map was generated using the IDW interpolation method.

The K factor is a quantitative measure of the soil's inherent resistance to erosion. This factor is estimated using the equation of Wischmeier and Smith (1978), as shown below (Eq. 3):

$$K = [2.1 \, M^{1.14} \times 10^{-4}(121a) + 3.25(b-2) + 2.5(c-3)] \times \frac{0.1317}{100} \quad (3)$$

where M = (% fine sand + silt)×(100 - % clay), a is the organic matter percentage, b is the code of permeability, c is the code of soil structure, and 0.1317 is a conversion factor from US units to international units.

The K factor was calculated using 20 soil samples

Table 1 Data from rainfall gauging stations in the Wadi El Hachem watershed

Items	Menaceur	Bellah	Bordj Ghobrini	Iazabene	Boukourdane's dam	Sidi Amar
Number of data years	46	41	44	44	28	22
Time period	1967-2012	1973-2013	1968-2011	1968-2011	1987-2014	1969-1990
Longitude (E,°)	2.23	2.24	2.26	2.28	2.30	2.30
Latitude (N,°)	36.49	36.61	36.60	36.47	36.54	36.56
Altitude (m)	250	20	15	420	110	45
Modified Fournier Index (mm)	88	99	123	158	105	121
Maximal daily rainfall (mm)	74	58	53	49	63	60
Annual average rainfall erosivity (MJ·mm·ha⁻¹·h⁻¹·yr⁻¹)	470	444	458	409	454	490

Table 2 Soil data of the Wadi El Hachem watershed

No.	Longitude (E,°)	Latitude (N,°)	Sand (%)	Clay (%)	Loam (%)	Texture	OM (%)	K(t·h ·MJ⁻¹·mm⁻¹)
1	2.23	36.50	42	30	28	Clay Loam	1.46	0.037
2	2.22	36.48	25	49	26	Clay	0.56	0.036
3	2.33	36.58	18	43	39	Clay	3.08	0.039
4	2.26	36.61	15	44	41	Silty Clay	3.06	0.039
5	2.29	36.54	29	27	44	Loam	2.20	0.035
6	2.26	36.53	24	49	27	Clay	0.83	0.032
7	2.29	36.55	44	28	28	Clay Loam	1.19	0.035
8	2.26	36.57	27	30	43	Clay Loam	3.19	0.038
9	2.31	36.60	20	38	42	Silty Clay Loam	0.58	0.041
10	2.34	36.60	40	19	41	Loam	2.86	0.046
11	2.27	36.45	54	13	33	Sandy Loam	2.98	0.027
12	2.16	36.47	23	35	42	Clay Loam	3.42	0.035
13	2.27	36.51	23	44	33	Clay	1.35	0.037
14	2.28	36.48	18	42	41	Silty Clay	1.39	0.042
15	2.32	36.56	38	27	35	Clay Loam	1.82	0.058
16	2.19	36.49	58	23	19	Sandy Clay Loam	1.10	0.039
17	2.30	36.51	18	41	41	Silty Clay	1.05	0.043
18	2.31	36.49	19	35	46	Silty Clay Loam	1.17	0.044
19	2.30	36.58	31	39	31	Clay Loam	1.61	0.034
20	2.27	36.59	5	51	43	Silty Clay	2.48	0.035

data collected from various locations throughout the watershed (Table 2). The soil sampling is of stratified random type based on lithological units distributed in the study region. The IDW interpolation method was used to create the K factor map.

The LS factor measures the erosion impact of slope angle, length, and complexity (Wall et al. 2002). To estimate LS factor through the watershed we used the Advanced Spaceborne Thermal Emission and Reflection Radiometer (ASTER) Global Digital Elevation Model (GDEM) with 30 m resolution. The LS factor is calculated according to the equation of Moore and Burch (1986) (Eq. 4).

$$LS = \left(\frac{A}{22.13}\right)^m \times \left(\frac{sin\beta}{0.0896}\right)^n \qquad (4)$$

where A is the upslope contributing area per unit contour width (m²m⁻¹), β is the slope angle in degrees, m = 0.4, and n = 1.3.

The C factor measures the effectiveness of vegetation cover and crop management systems in reducing soil loss (Panagos et al. 2015). The C factor can be estimated using a variety of methods (Almagro et al. 2019). Several studies over the last few decades have focused on using Normalized Difference Vegetation Index (NDVI) as an independent variable to estimate this factor (Van der Knijff et al. 2000; Panagos et al. 2015). In our study, the generation of the C factor map is obtained using the equation of (Durigon et al. 2014) (Eq. 5):

$$C = \left(\frac{-NDVI + 1}{2}\right) \qquad (5)$$

where NDVI = (NIR-RED)/(NIR+RED), NIR is the near infrared band of the Landsat 8 OLI satellite image (band 5), and RED is the red band of the Landsat 8 OLI satellite image (band 4).

In our example, we calculated an average NDVI

derived from different Landsat 8 OLI satellite images at 0% cloud cover for the year 2018.

The P factor takes into account the effectiveness of soil conservation practices in reducing erosion. Contour farming, cross-slope cultivation and strip cropping are the most widely used conservation practices (Stone and Hilborn 2000). In our study area, only 0.13% of the total watershed area is used for conservation practices (Saoud and Meddi 2022). Consequently, the whole watershed was assigned a value of 1.

3.2 Sediment yield calculation

The sediment yield (SY) is defined as the part of soil eroded and deposited towards the outlet of a watershed (Ebrahimzadeh et al. 2018). The average SY can be calculated using the following formula (Eq. 6):

$$SY = SDR \times A \qquad (6)$$

where SDR is the sediment delivery ratio (dimensionless), and A is the average soil loss of the watershed (t·ha^{-1}·yr^{-1}).

There are two sorts of SDR models based on their input data: those based on the drainage area and those based on the morphometric features of the watershed (Bhattacharya and Das Chatterjee 2021). In our study, SY was estimated using four (04) SDR models (Table 3). To select the best model, we compared the SY derived from each of the four SDR models (SY$_{est}$) to the SY observed at the outlet of the watershed (SY$_{obs}$). The criteria used are standard error (SE) (Eq. 7), standard deviation (SD) (Eq. 8), coefficient of variation (CV) (Eq. 9) (Rostami and Salajeghe 2011; Boufeldja et al. 2020), and the Nash–Sutcliffe efficiency (NSE) (Eq. 10) (Nash and Sutcliffe 1970). The best model is chosen by having the lowest SE, SD, and CV, as well as the greatest NSE.

$$SE = \frac{|SY_{est} - SY_{obs}|}{SY_{est}} \times 100 \qquad (7)$$

$$SD = \sqrt{\frac{(SY_{est} - SY_{obs})^2}{SY_{obs}}} \qquad (8)$$

$$CV = \frac{SD}{SY_{obs}} \times 100 \qquad (9)$$

$$NSE = 1 - \frac{(SY_{obs} - SY_{est})^2}{SY_{obs}^{2}} \qquad (10)$$

where SE is the standard error (%), SD is the standard deviation, CV is the coefficient of variation (%), NSE is the Nash–Sutcliffe efficiency, SY$_{est}$ is the sediment yield estimated from Eq. 6, and SY$_{obs}$ is the sediment yield observed at the catchment outlet.

4 Results

4.1 RUSLE factors

The factors of soil loss described in the RUSLE model were studied to better understand the intensity and geographical distribution of this process across the study area. The R factor values were in the range of 408 to 490, indicating a high level of rainfall erosivity. The highest values were located in the north of the watershed and they gradually decrease towards the south (Fig. 4). The results of K factor were between 0.027 and 0.058. The highest readings indicating a very high level of erodibility (between 0.0394 and 0.058) were located in the north and east of the watershed, while those showing very low erodibility (less than 0.0332) were found in the south (Fig. 5). This result highlighted the effect of soil intrinsic properties on K factor. It is noted that sites with very high erodibility had either low organic matter content (case of site 9), or high silt content (case of site 14 and 17), or both at the same time (case of site 15) (Table 2). However, there were sites with high silt content but low K values. This is due to

Table 3 Different SDR models used for the calculation of SY$_{est}$

| SDR models	Source	Description
$SDR = 1.8768 - 0.4191 \times \log(25.89\,A)$	Maner (1962)	A: Watershed area (km²)
$SDR = 0.42 \times 2.589\,A^{-0.125}$	Vanoni (1975)	A: Watershed area (km²)
$SDR = 0.417762 \times 2.589\,A^{-0.134958} - 0.127097$	SCS (1983)	A: Watershed area (km²)
$\log(SDR) = 2.94259 + 0.82362 \times \log\left(\frac{R}{L}\right)$	Renfro (1983)	R: Maximum height of the watershed - height at the outlet (km) L: Maximum length of the watershed measured parallel to the main watercourse (km)
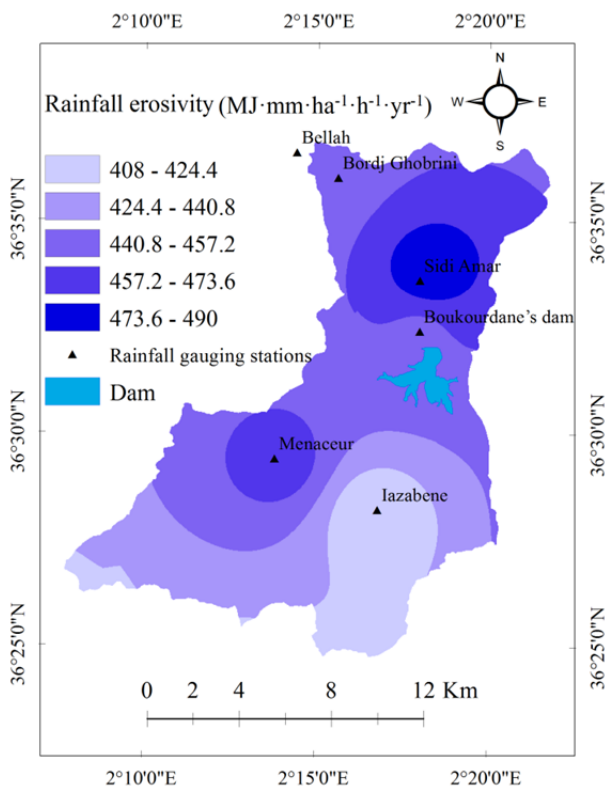
Fig. 4 Rainfall erosivity factor map for the Wadi El Hachem watershed.

relatively high levels of organic matter (sites 5, 8 and 12). Like organic matter, sand played an important role in reducing soil erodibility. This was particularly apparent at sites 7, 11 and 16, where the percentage of sand was greater than or equal to 44% while K was less than 0.039. The LS factor values ranged from 0 to 65. The irregularity of the slope length and its inclination influenced the LS factor distribution in the watershed (Fig. 6). Indeed, the highest values were located in the vast areas with regular slopes, i.e. floodplains, depressions and plateaus with gentle slopes, while the lowest values were located in areas with irregular slopes and in flat lands with no slope. The C factor values were between 0.072 and 0.58. The C factor classes were recognized based on land use type (Fig. 7). The class below 0.173 was represented by forests. It was mainly located in the southern part of the watershed, but was also found in the central and northern parts of the watershed. The 0.173 to 0.274 class represented shrubs and farmlands. The values between 0.274 and 0.376 were represented by rangelands, fallows and burned forests. Finally, built-up areas and bare soils were represented by the class greater than 0.376.
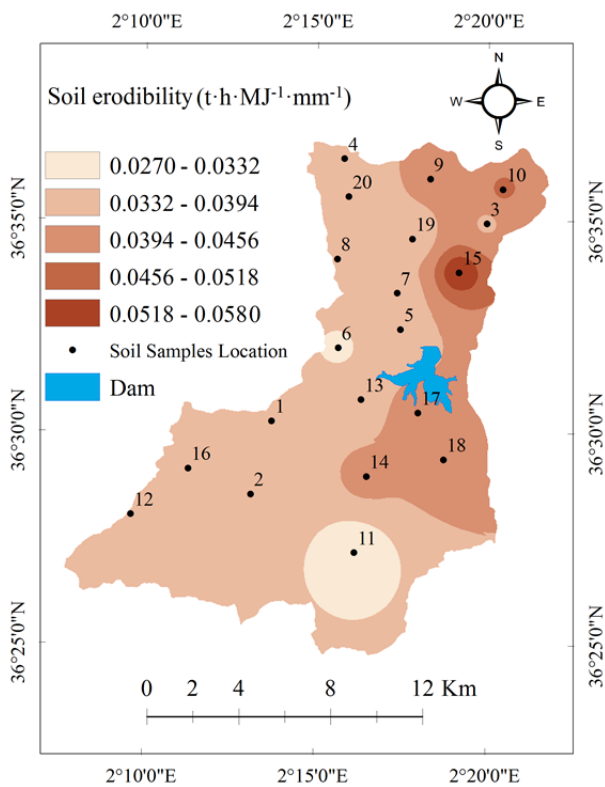

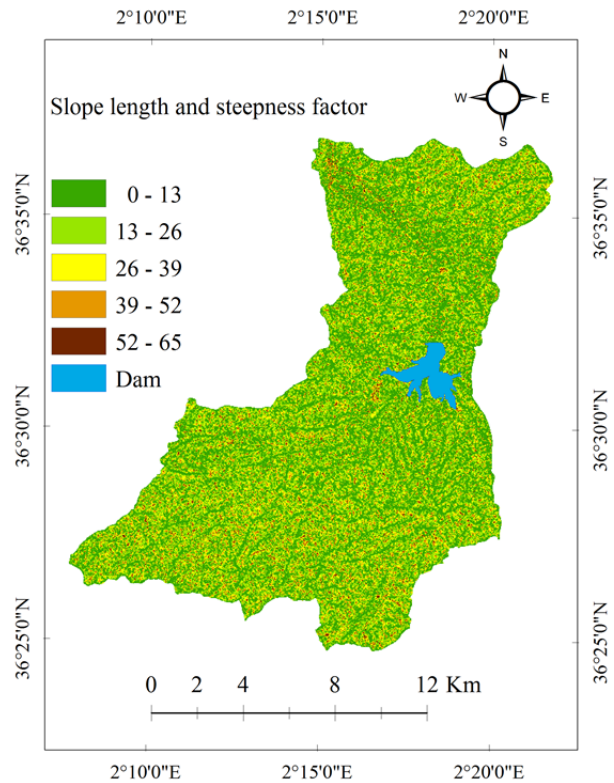**Fig. 5** Soil erodibility factor map for the Wadi El Hachem watershed.

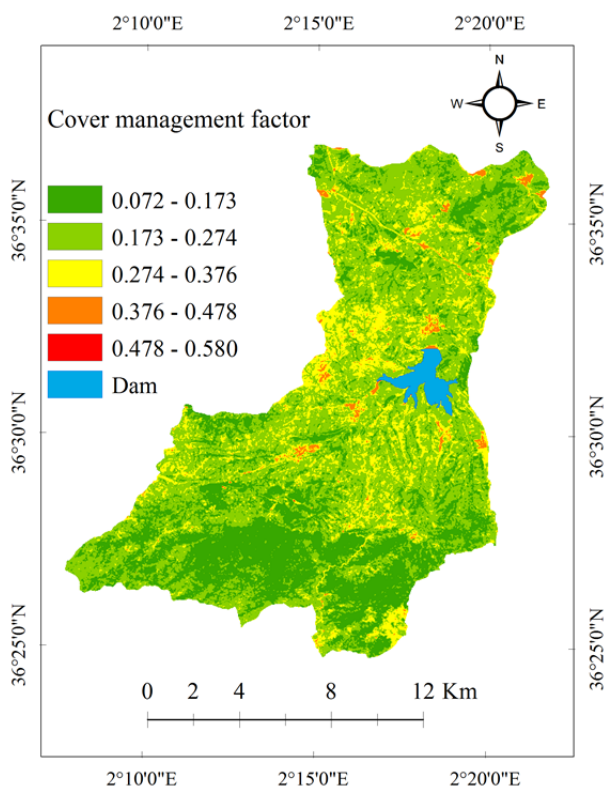**Fig. 6** Slope length and steepness factor map for the Wadi El Hachem watershed.

Fig. 7 Cover management factor map for the Wadi El Hachem watershed.

4.2 Soil loss, SDR, and sediment yield

A derived from the RUSLE model were between 0 and 410. The distribution of A in the map (Fig. 7) showed that low values (less than 30 t·ha⁻¹·yr⁻¹) were found in areas occupied by forests, particularly in the South, where climatic aggressiveness is relatively low. The highest soil losses (more than 120 t·ha⁻¹·yr⁻¹) were located in the floodplains, specifically at the outlet of the watershed and west of the dam. They were also found in bare soils and burnt areas. The annual average soil loss in the Wadi El Hachem watershed was 52 t·ha⁻¹·yr⁻¹.

The comparison of the sediment yield estimated (SY_{est}) derived from the RUSLE-SDR results with the sediment yield observed (SY_{obs}) involved the selection of the most appropriate sediment delivery ratio (SDR) model. This selection was based on the lowest rates of standard error (SE), standard deviation (SD), and coefficient of variation (CV), as well as the highest rate of the Nash–Sutcliffe efficiency (NSE). SY_{obs} was derived from a bathymetric survey of the Boukourdane's

dam conducted by the National Agency for Dams and Transfers (ANBT) in 2005, as well as forecasts of siltation evolution using the Chamov formula (Demmak 2010). According to Saoud and Meddi (2022), and depending on the results of Remini and Mokeddem (2018), about the annual siltation rate of the Boukourdane's dam, the SY_{obs} in the Wadi El Hachem watershed was predicted to be 27 t·ha⁻¹·yr⁻¹. Table 4 showed that the SY_{est} values ranged from 6 to 36 t·ha⁻¹·yr⁻¹. It can be seen that the SY_{est} derived from the model of Renfro (1983) was the closest to SY_{obs}. In fact, SY_{est} was about 27 t·ha⁻¹·yr⁻¹ with SE, SD, CV and NSE of 0.38, 0.02, 0.07 and 1.00, respectively. Similarly, Fig. 8 clearly illustrated that Renfro's model was the best of the four models tested that produced similar findings when compared to the observed data. After selecting the suitable SDR model and using the Eq. 6, the sediment yield (SY) map for the entire Wadi El Hachem watershed was developed using Renfro's SDR model and the soil loss (A) value for each pixel (Fig. 9). According to the map, sediment production areas were mainly concentrated in the Northeast of the basin, at the outlet of the basin, and in the tributaries of the dam.

Table 4 Results of SDR models and SY_{est}

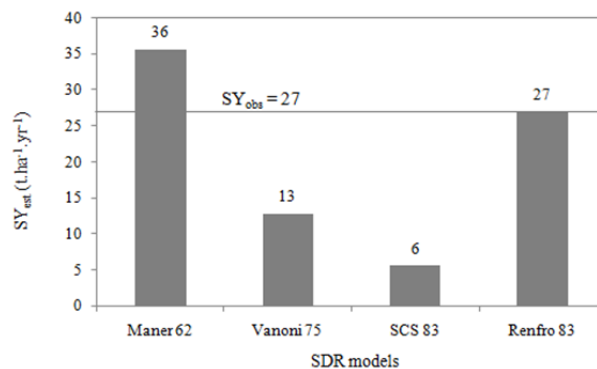| SDR models	SDR	SY_{est}	SE (%)	SD	CV (%)	NSE
Maner (1962)	0.69	36	24.29	1.67	6.16	0.90
Vanoni (1975)	0.25	13	110.54	2.73	10.08	0.72
SCS (1983)	0.11	6	377.86	4.12	15.18	0.37
Renfro (1983)	0.52	27	0.38	0.02	0.07	1.00

Fig. 8 Sediment yield estimated from Sediment Delivery Ratio (SDR) models vs sediment yield observed.

4.3 Soil loss (A) and sediment yield (SY) simulations in dry and rainy years

To investigate the importance of the rainfall erosivity (R) factor and its impact on soil loss (A)
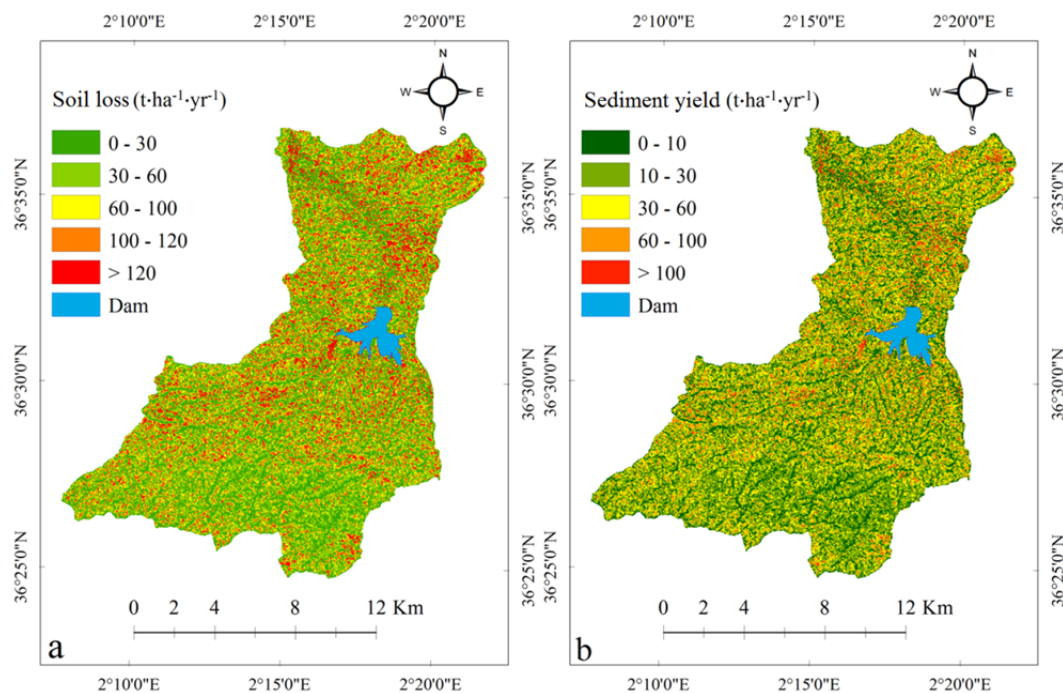
Fig. 9 Spatial distribution of the average annual soil loss (a) and sediment yield (b).

and sediment yield (SY), the RUSLE-SDR model was used to estimate A and SY for both dry and rainy years. This was obtained by varying the values of the R factor, while keeping the other factors constant. Dry and rainy years were selected from the data of the six (06) rain gauging stations, and each station was treated separately. Thus, years with the lowest precipitation (P) (mm) were considered dry years and years with the highest P (mm) were considered rainy years. Table 5 showed that during the rainy year, soil loss and sediment yield were higher than average (60 and 31 versus 52 and 27, respectively); whereas they were lower than average during the dry year (45 and 23 versus 52 and 27, respectively). This result become clear when compared to the values of rainfall erosivity and precipitation which rose from the dry year to the average and then to the rainy year (Table 5). In fact, the mean R in the three situations was 149, 414, and 820 MJ·mm·ha^{-1}·yr^{-1}, respectively. The same behaviour may be seen in the case of the mean precipitation (245, 532, and 832 mm, respectively). The difference in rainfall erosivity and precipitation between dry and rainy years was 671 and 587, respectively. As a result of this fluctuation, soil loss and sediment yield had increased by 15 and 8 t·ha^{-1}·yr^{-1}, respectively. This finding implied that rainfall erosivity had a serious effect on erosion and sediment yield. Fig. 10 and

Table 6 go into further detail about the difference between dry and rainy years. Indeed, the distribution of the soil loss in the dry year showed that the class less than 30 t·ha^{-1}·yr^{-1} occurred in 76% of the catchment area. However, in the rainy year, this class accounted for just 27% of the catchment area, whereas the class greater than 100 t·ha^{-1}·yr^{-1} accounted for 45% of the watershed area. In the case of sediment yield, the class below 10 t·ha^{-1}·yr^{-1} accounted for 63% of the basin in the dry year, but just 24% in the rainy year. However, the class greater than 30 t·ha^{-1}·yr^{-1} in the rainy year covered 61% of the basin, up from 7% in the dry year.

Table 5 Soil loss and sediment yield in average, dry year, and rainy year

Period	A	SY	R	P
Average	52	27	414	532
Dry year	45	23	149	245
Rainy year	60	31	820	832

Note: A is average annual soil loss (t·ha^{-1}·yr^{-1}); SY is sediment yield (t·ha^{-1}·yr^{-1}); R is rainfall erosivity (MJ·mm·ha^{-1}·h^{-1}·yr^{-1}); P is precipitation (mm).

5   Discussion

The RUSLE model findings highlighted the impact of each factor on the intensity and distribution of soil loss across the watershed. Moreover, the areas
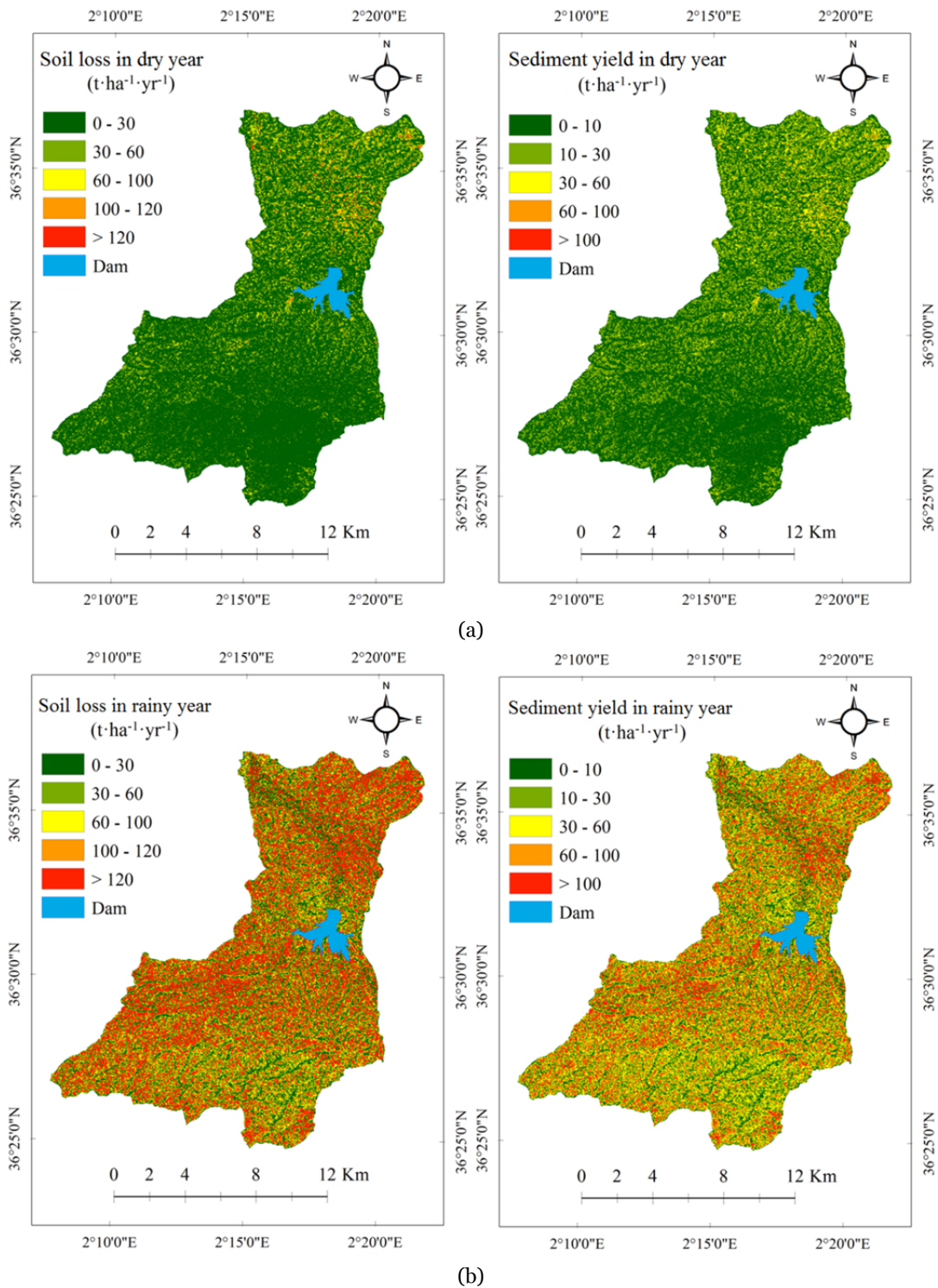
Fig. 10 Spatial distribution of the soil loss and sediment yield in dry year (a) and rainy year (b).

with the highest potential for soil loss are those with high levels of one or more RUSLE factors and vice versa. In fact, the high rates of soil loss at the basin outlet and in the dam's tributaries are caused by high LS factor values (LS> 52). Similarly, areas with values greater than 120 t·ha⁻¹·yr⁻¹ in the north-east of the watershed are related to high rates of R and K factors, and those which are situated in the centre and south of the basin are related to high rates of C factor. In the same way, the lowest erosion values reported in flat

lands are mainly due to the LS factor's behaviour in these areas. On the other hand, the inverse effect of one factor among others can affect the erosive potential. Indeed, despite the fact that the LS factor is high in the south of the watershed due to the complexity of the topography, the presence of dense vegetation has reduced the erosive potential. Furthermore, despite the presence of forest lands in the extreme south of the watershed, forest fires have highlighted the intensity of the erosive potential.

Table 6 Distribution of average annual soil loss (A) and sediment yield (SY) classes in dry year and rainy year

Area of A (%)			Area of SY (%)		
Classes	Dry year	Rainy year	Classes	Dry year	Rainy year
0 - 30	76	27	0 - 10	63	24
30 - 60	17	12	10 - 30	30	14
60 - 100	5	17	30 - 60	6	24
100 - 120	1	8	60 - 100	1	20
> 120	1	37	> 100	0	17

The average soil loss estimated by the RUSLE model is 2.6 times higher than the sheet and rill erosion rate recorded at the scale of the experimental plots, which can reach 20 t·ha⁻¹·yr⁻¹ in the Mediterranean mountains (Roose et al. 2000). However, it is in the range of specific degradation recorded from hydrometric stations and dams distributed in Northern Algeria, which varies from 0.64 to 76.20 t·ha⁻¹·yr⁻¹ (Meddi 2015). In Mediterranean mountains, where the study area is located, linear erosion is much more effective than sheet and rill erosion, as reported by (Roose et al. 2000). The RUSLE model can estimate erosive potential at any location in space at the watershed scale. However it is solely meant to predict sheet and rill erosion, which corresponds to lands of less than 20% slope (Wischmeier and Smith 1978). In our situation, however, land with a slope of less than 20% accounts for only 36% of the watershed. This RUSLE model feature is one of the reasons behind the obtained outcome. Another possible explanation for this finding is the combined influence of climate and relief. Meddi et al. (2016) found that the coastal region of Algeria specifically from the centre to the East, where the research zone is located, is characterized by high rainfall erosivity values. According to Demmak (1982), rainfall in the Mediterranean environment can be dangerous in the form of violent storms. Aside from the climatic influence, relief plays an important function in

emphasizing the erosive potential. According to Mostephaoui et al. (2013), water erosion affects 14 million hectares in Algeria, primarily in mountainous areas. In the Wadi El Hachem watershed, more than 64% of the land has a slope greater than 20%, making the area particularly prone to water erosion. Water erosion can also be influenced by soil properties. In Algeria, Badreddine et al. (2021) found that soil intrinsic characteristics such as texture and organic content have a substantial impact on soil sensitivity, which can affect soil erosion. In a more in-depth investigation, Khanchoul and Boubehziz (2019) found that the K factor was negatively correlated with clay content, soil permeability, and organic matter (r = -0.72, -0.64 and -0.48, respectively), while it was positively correlated with silt and sand content and soil structure (r= 0.48, 0.42 and 0.21, respectively). In terms of the C factor which is affected by land use type, built-up areas and bare soils are by far the most affected by the erosive process, whereas forests are the least affected. This outcome is consistent with previous studies on the same topic. According to El Jazouli et al. (2019), the most prominent causes of erosion caused by land use change are deforestation and conversion of land to built-up areas. Similarly, Ghosh et al. (2022) found that vegetated areas limit the intensity of surface runoff and increase the infiltration process, whereas built-up areas substantially inhibit water penetration into the soil and accelerate surface runoff. The average soil loss reported in the Wadi El Hachem watershed is nearly equivalent to other studies in the Mediterranean basin with similar conditions to the study area such as Tribak et al. (2012, 61.42 t·ha⁻¹·yr⁻¹), Lelandais and Fabre (1996, 60 t·ha⁻¹·yr⁻¹), Sadiki et al. (2004, 55.35 t·ha⁻¹·yr⁻¹), Farhan and Nawaiseh (2015, 64 t·ha⁻¹·yr⁻¹), and El Hage Hassan et al. (2018, 46 t·ha⁻¹·yr⁻¹).

In order to predict SY, an accurate estimation of SDR coupling with RUSLE findings is crucial. The best strategy for calculating SY in our investigation was to employ SDR based on Renfro's model, out of the four SDR models used. This model is based on morphometric properties of the watershed, such as the watershed's maximum height, height at the outlet, and maximum length measured parallel to the main watercourse. As a result of this finding, we can deduce that in our case, the best SDR prediction models are those based on the basin's morphometric properties, rather than the drainage area. This finding is in line with previous studies on the same topic (Onyando et

al. 2005; Kidane et al. 2019; Tsegaye and Bharti 2021). However, other studies show that the drainage area is the most accurate measure for estimating the SDR (Colman et al. 2018; Ebrahimzadeh et al. 2018; Thomas et al. 2018). According to the SDR value it can be seen that 52% of the eroded soil can reach the flow system, and hence the watershed's outlet. This result is comparable to other works such as Fu et al. (2006, SDR=0.437), Behera et al. (2020, SDR is between 0.22 and 0.54), Ouadja et al. (2022, SDR is between 0.23 and 0.56) and Swarnkar et al. (2018, SDRs are 0.45 and 0.63). However, it may be relatively high compared to the results of other works (Hui et al. 2010; Bhattacharya and Das Chatterjee 2021; Ben Cheikha et al. 2021) (SDRs are between 0.19 and 0.206). This may be due to each of two factors. The first one is relatively limited size of our study area. The second one is the watershed's hilly and rugged environment. Ferro and Minacapilli (1995) revealed that SDR is often inversely proportional to basin area. In the same way, Bhattacharya et al. (2020) noticed that SDR is lower in watersheds with larger drainage areas because vast regions have a higher possibility of trapping sediment, whereas the probability of sediment reaching the stream is low. Tsegaye and Bharti (2021) also noticed that slopes that are short and steep provide more sediment than longer and levelled ones.

The simulation results of the soil loss and sediment yield in dry and rainy years, revealed that the rainfall erosivity is one of the main factors affecting soil erosion, in the Wadi El Hachem watershed. In reality, a rainy year is distinguished by more frequent and intense precipitation, which causes an increase in soil water content, reduced infiltration rates, and increased runoff (Ben Cheikha et al. 2021). Therefore, surface runoff is a consequence of a high precipitation and rainfall erosivity rates, particularly in mountainous areas, where the impact of slope on erosion and sediment yield is amplified. Meddi et al. (2016) reported that surface runoff is a significant erosion-causing factor in mountainous environments.

6 Conclusion

The RUSLE-SDR model is used to accomplish the following aims: (i) estimating the average annual soil loss (A) and sediment yield (SY) in the Wadi El Hachem watershed, (ii) mapping the RUSLE factors as well as A and SY, and (iii) examining the influence of rainfall erosivity (R) on soil erosion and sediment yield in dry and wet years. The soil loss results range from 0 to 410 t·ha^{-1}·yr^{-1}, with an annual average of 52 t·ha^{-1}·yr^{-1}. The Renfro (1983) model was chosen as the best SDR model for calculating SY, with standard error (SE), standard deviation (SD), coefficient of variation (CV), and Nash–Sutcliffe efficiency (NSE) values of 0.38, 0.02, 0.07, and 1.00, respectively. The average SY in the entire watershed is about 27 t·ha^{-1}·yr^{-1}. The SY map for the whole watershed revealed that sediment production zones are mostly concentrated in the Northeast of the basin, at its outlet, and in the tributaries of the dam. The combined effect of climate and topography was clearly seen in the results of A and SY. The findings of A and SY simulation in dry and rainy years showed that R is one of the main factors affecting soil erosion in the Wadi El Hachem watershed. The mean difference in R between dry and rainy years is 671 MJ·mm·ha^{-1}·h^{-1}·yr^{-1}. As a result of this variation, A and SY have increased by 15 and 8 t·ha^{-1}·yr^{-1}, respectively. The findings of this study may be used to provide scientific and technical support for the Wadi El Hachem watershed's conservation and management plans.

Acknowledgments

References

Alewell C, Borrelli P, Meusburger K, Panagos P (2019) Using the USLE: Chances, challenges and limitations of soil erosion modelling. Int Soil Water Conserv Res 7:203−225. https://doi.org/10.1016/j.iswcr.2019.05.004

Almagro A, Thomé TC, Colman CB, et al. (2019) Improving cover and management factor (C-factor) estimation using remote sensing approaches for tropical regions. Int Soil Water Conserv Res 7:325−334. https://doi.org/10.1016/J.ISWCR.2019.08.005

Badreddine B, Mohammed H, Boutkhil M, et al. (2021) Assessment of erosion: use of nuclear techniques and conventional methods—case of the Fergoug watershed,

Algeria. Environ Monit Assess 193:55.
https://doi.org/10.1007/s10661-020-08826-w

Behera M, Sena DR, Mandal U, et al. (2020) Integrated GIS-based RUSLE approach for quantification of potential soil erosion under future climate change scenarios. Environ Monit Assess 2020 19211 192:1–18.
https://doi.org/10.1007/S10661-020-08688-2

Ben Cheikha L, Jaoued M, Aouadi T, et al. (2021) Quantifying of water erosion and sediment yield by SEAGIS model in Rmel watershed (north-eastern Tunisia). Environ Earth Sci 2021 8024 80:1–13.
https://doi.org/10.1007/S12665-021-10103-Z

Benchettouh A, Kouri L, Jebari S (2017) Spatial estimation of soil erosion risk using RUSLE/GIS techniques and practices conservation suggested for reducing soil erosion in Wadi Mina watershed (northwest, Algeria). Arab J Geosci 10:79.
https://doi.org/10.1007/s12517-017-2875-6

Bhandari KP, Aryal J, Darnsawasdi R (2015) A geospatial approach to assessing soil erosion in a watershed by integrating socio-economic determinants and the RUSLE model. Nat Hazards 75:321–342.
https://doi.org/10.1007/s11069-014-1321-2

Bhattacharya RK, Chatterjee ND, Das K (2020) Estimation of erosion susceptibility and sediment yield in ephemeral channel using rusle and sdr model: Tropical plateau fringe region, india. Adv Sci Technol Innov 163–185.
https://doi.org/10.1007/978-3-030-23243-6_10

Bhattacharya RK, Das Chatterjee N (2021) Fluvial sediment budget and mining impact assessment: Use of RUSLE, SDR and hydraulic models. Environ Sci Eng 51–104.
https://doi.org/10.1007/978-3-030-72296-8_3

Boufeldja S, Baba Hamed K, Bouanani A, et al. (2020) Identification of zones at risk of erosion by the combination of a digital model and the method of multi-criteria analysis in the arid regions: case of the Bechar Wadi watershed. Appl Water Sci 10:121.
https://doi.org/10.1007/s13201-020-01191-6

Chafai A, Brahim N, Shimi NS (2020) Mapping of water erosion by GIS/RUSLE approach: watershed Ayda river—Tunisia study. Arab J Geosci 13:810.
https://doi.org/10.1007/s12517-020-05774-0

Colman CB, Garcia KMP, Pereira RB, et al. (2018) Different approaches to estimate the sediment yield in a tropical watershed. Rbrh 23:.
https://doi.org/10.1590/2318-0331.231820170178

Demmak A (2010) Realization of the updating study of the national water plan in Algeria. Mission 2 : Resources and demands. Volume 3 : Siltation of dams. (In French)

Demmak A (1982) Contribution to the study of erosion and solid transport in northern Algeria. (In French)

Djoukbala O, Mazour M, Hasbaia M, et al. (2018) Estimating of water erosion in semiarid regions using RUSLE equation under GIS environment. Environ Earth Sci 77:345.
https://doi.org/10.1007/s12665-018-7532-1

Durigon VL, Carvalho DF, Antunes MAH, et al. (2014) NDVI time series for monitoring RUSLE cover management factor in a tropical watershed. Int J Remote Sens 35:441–453.
https://doi.org/10.1080/01431161.2013.871081

Ebrahimzadeh S, Motagh M, Mahboub V, et al. (2018) An improved RUSLE/SDR model for the evaluation of soil erosion. Environ Earth Sci 77:454.
https://doi.org/10.1007/s12665-018-7635-8

El Hage Hassan H, Charbel L, et al. (2018) Modeling water erosion at the scale of the Mhaydssé watershed. Bekaa-Lebanon. [VertigO] La Rev électronique en Sci l'environnement 18:.
https://doi.org/10.4000/vertigo.19804. (In French)

El Jazouli A, Barakat A, Khellouk R, et al. (2019) Remote sensing and GIS techniques for prediction of land use land cover change effects on soil erosion in the high basin of the Oum Er Rbia River (Morocco). Remote Sens Appl Soc Environ 13:361–374.
https://doi.org/10.1016/j.rsase.2018.12.004

FAO, ITPS (2015) Status of the World's Soil Resources (SWSR) - Main Report. Food and Agriculture Organization of the United Nations.

Farhan Y, Nawaiseh S (2015) Spatial assessment of soil erosion risk using RUSLE and GIS techniques. Environ Earth Sci 74:4649–4669.
https://doi.org/10.1007/s12665-015-4430-7

Ferreira CSS, Seifollahi-Aghmiuni S, Destouni G, et al. (2022) Soil degradation impact on soil erosion in the European Mediterranean region: Processes, status and consequences. Sci Total Environ 805:150106.
https://doi.org/10.1016/j.scitotenv.2021.150106

Ferro V, Minacapilli M (1995) Sediment delivery processes at basin scale. Hydrol Sci Sci Hydrol 40:703.
https://doi.org/10.1080/02626669509491460

Fu G, Chen S, McCool DK (2006) Modeling the impacts of no-till practice on soil erosion and sediment yield with RUSLE, SEDD, and ArcView GIS. Soil tillage Res 85:38–49.
https://doi.org/10.1016/j.still.2004.11.009

Ghosh D, Banerjee M, Karmakar M, et al. (2022) Application of Geoinformatics and AHP Technique to Delineate Flood Susceptibility Zone: A Case Study of Silabati River Basin, West Bengal, India BT - Geospatial Technology for Environmental Hazards: Modeling and Management in Asian Countries. In: Shit PK, Pourghasemi HR, Bhunia GS, et al. (eds). Springer International Publishing, Cham. pp 97–130.

Hui L, Xiaoling C, Lim KJ, et al. (2010) Assessment of soil erosion and sediment yield in Liao watershed, Jiangxi Province, China, Using USLE, GIS, and RS. J Earth Sci 21:941–953.
https://doi.org/10.1007/s12583-010-0147-4

Jaafari Y, Benabdelhadi M (2020) Assessment of Rainfall Soil Loss in Allal El Fassi Watershed (Mean Atlas Morocco) Using RUSLE Method Combining to GIS and Remote Sensing. In: Geospatial Technology. Springer, pp 95–103

Jain MK, Das D (2009) Estimation of sediment yield and areas of soil erosion and deposition for watershed prioritization using GIS and remote sensing. Water Resour Manag 2009 2410 24:2091–2112.
https://doi.org/10.1007/S11269-009-9540-0

Khanchoul K, Boubehziz S (2019) Spatial variability of soil erodibility at el hammam catchment, northeast of algeria. Environ Ecosyst Sci 3:17–25

Kidane M, Bezie A, Kesete N, et al. (2019) The impact of land use and land cover (LULC) dynamics on soil erosion and sediment yield in Ethiopia. Heliyon 5:e02981.
https://doi.org/10.1016/j.heliyon.2019.e02981

Kumar S (2020) Geospatial Applications in Modeling Climate Change Impact on Soil Erosion. In: Venkatramanan V, Shah S, Prasad R (eds.), Global Climate Change: Resilient and Smart Agriculture. Springer Singapore, Singapore, pp 249–27.

Lelandais F, Fabre G (1996) Anti-erosion management plan of the Ouergha wadi watershed (Morocco), Erosion risks and geographic information systems. Bull Réseau Eros 16:439–443. (In French)

López-Vicente M, Navas A, Machín J (2008) Identifying erosive periods by using RUSLE factors in mountain fields of the Central Spanish Pyrenees. Hydrol Earth Syst Sci 12:523–535.
https://doi.org/10.5194/hess-12-523-2008

Magesh NS, Chandrasekar N (2016) Assessment of soil erosion and sediment yield in the Tamiraparani sub-basin, South India, using an automated RUSLE-SY model. Environ Earth Sci 75:1208.
https://doi.org/10.1007/s12665-016-6010-x

Maner SB (1962) Factors influencing sediment delivery ratios in the Blackland Prairie land resource area. US Dept. of Agriculture, Soil Conservation Service, Texas, USA.

Meddi M (2015) Contribution to the study of solid transport in northern Algeria. LARHYSS J 315–336. (In French)

Meddi M, Toumi S, Assani AA (2016) Spatial and temporal variability of the rainfall erosivity factor in Northern Algeria. Arab J Geosci 9:282–294.
https://doi.org/10.1007/s12517-015-2303-8

Meghraoui M, Habi M, Morsli B, et al. (2017) Mapping of soil erodibility and assessment of soil losses using the RUSLE model in the Sebaa Chioukh Mountains (northwest of Algeria). J water L Dev 34:205–213.

https://doi.org/10.1515/jwld-2017-0055

Menasria A, Meddi M, Habaieb H (2021) Mapping the risk of soil erosion in the Medjerda and Mellegue Catchments using the RUSLE Model, Remote Sensing, and GIS. Taiwan Water Conserv 69:12–39. https://doi.org/10.6937/TWC.202112/PP_69(4).0002

Merritt WS, Letcher RA, Jakeman AJ (2003) A review of erosion and sediment transport models. Environ Model Softw 18:761–799. https://doi.org/10.1016/S1364-8152(03)00078-1

Moore ID, Burch GJ (1986) Modelling erosion and deposition: topographic effects. Trans ASAE 29:1624–1630. https://doi.org/10.13031/2013.30363

Mostephaoui T, Merdas S, Sakaa B, et al. (2013) Mapping of water erosion risks by application of the universal soil loss equation using a geographic information system in the El Hamel Watershed (Boussaada) Algeria. J Algérien des Régions Arid N° Spécial 12:131–147. (In French)

Mukanov Y, Chen Y, Baisholanov S, et al. (2019) Estimation of annual average soil loss using the Revised Universal Soil Loss Equation (RUSLE) integrated in a Geographical Information System (GIS) of the Esil River basin (ERB), Kazakhstan. ACTA Geophys 67:921–938. https://doi.org/10.1007/s11600-019-00288-0

Nash JE, Sutcliffe JV (1970) River flow forecasting through conceptual models part I — A discussion of principles. J Hydrol 10:282–290. https://doi.org/10.1016/0022-1694(70)90255-6

Nasir N, Selvakumar R (2018) Influence of land use changes on spatial erosion pattern, a time series analysis using RUSLE and GIS: the cases of Ambuliyar sub-basin, India. ACTA Geophys 66:1121–1130. https://doi.org/10.1007/s11600-018-0186-2

Onyando JO, Kisoyan P, Chemelil MC (2005) Estimation of potential soil erosion for river Perkerra catchment in Kenya. Water Resour Manag 19:133–143. https://doi.org/10.1007/S11269-005-2706-5

Osman KT (2014) Soil Erosion by Water. In: Soil Degradation, Conservation and Remediation. Springer Netherlands, Dordrecht, pp 69–101

Ouadja A, Benfetta H, Porto P, et al. (2022) GIS and remote sensing integration for sediment performance assessment based on a RUSLE and sediment delivery ratio model in northwest Algeria. Arab J Geosci 15:1–21. https://doi.org/10.1007/s12517-022-09502-8

Panagos P, Borrelli P, Meusburger K, et al. (2015) Estimating the soil erosion cover-management factor at the European scale. Land use policy 48:38–50. https://doi.org/10.1016/J.LANDUSEPOL.2015.05.021

Phinzi K, Ngetar NS (2019) The assessment of water-borne erosion at catchment level using GIS-based RUSLE and remote sensing: A review. Int Soil Water Conserv Res 7:27–46. https://doi.org/10.1016/j.iswcr.2018.12.002

Rajbanshi J, Bhattacharya S (2020) Assessment of soil erosion, sediment yield and basin specific controlling factors using RUSLE-SDR and PLSR approach in Konar river basin, India. J Hydrol 124935. https://doi.org/10.1016/j.jhydrol.2020.124935

Remini B, Mokeddem FZ (2018) Boukourdane (Algeria): a reservoir dam with low siltation rate. LARHYSS J 35:29–44

Renfro R, Waldo P (1983) Validations of sediment delivery ratio Prediction techniques. Research paper, p 95.

Roose E, Chebbani R, Bourougaa L (2000) Ravinement in Algeria. Typology, control factors, quantification and rehabilitation. Sci Chang planétaires/Sécheresse 11:317–326. (In French)

Rostami N, Salajeghe A (2011) Selecting the best model of Sediment Delivery Ratio estimation in Ilam dam basin. Adv Environ Biol 5:795–802

Sadiki A, Bouhlassa S, Auajjar J, et al. (2004) Use of a GIS for the evaluation and mapping of erosion risks by the Universal Soil Loss Equation in the Eastern Rif (Morocco): case of the oued Boussouab watershed. Bull l'Institut Sci Rabat, Sect Sci la Terre 26:69–79. (In French)

Sahli Y, Mokhtari E, Merzouk B, et al. (2019) Mapping surface water erosion potential in the Soummam watershed in Northeast Algeria with RUSLE model. J Mt Sci 16:1606–1615. https://doi.org/10.1007/s11629-018-5325-3

Saoud M, Meddi M (2022) Mapping of erosion using USLE, GIS and remote sensing in Wadi El Hachem Watershed (Northern Algeria): Case study. J Indian Soc Remote Sens 50:569–581. https://doi.org/10.1007/s12524-021-01481-9

Saygın SD, Ozcan AU, Basaran M, et al. (2014) The combined RUSLE/SDR approach integrated with GIS and geostatistics to estimate annual sediment flux rates in the semi-arid catchment, Turkey. Environ Earth Sci 71:1605–1618. https://doi.org/10.1007/s12665-013-2565-y

Schmidt S, Alewell C, Meusburger K (2019) Monthly RUSLE soil erosion risk of Swiss grasslands. J Maps 15:247–256. https://doi.org/10.1080/17445647.2019.1585980/SUPPL_FILE/TJOM_A_1585980_SM9601.ZIP

Singh AK, Kumar S, Naithani S, et al. (2019) Soil erosion and sediment yield estimation using remote sensing data and GIS in a Sitlarao watershed of north-western Himalayan region. Indian J Soil Conserv 47:143–154

Stone RP, Hilborn D (2000) Universal soil loss equation (USLE). Ontario Ministry of Agriculture. Food Rural Aff, Ontario, Canada, p 9.

Swarnkar S, Malini A, Tripathi S, et al. (2018) Assessment of uncertainties in soil erosion and sediment yield estimates at ungauged basins: an application to the Garra River basin, India. Hydrol Earth Syst Sci 22:2471–2485. https://doi.org/10.5194/hess-22-2471-2018

Thomas J, Joseph S, Thrivikramji KP (2018) Assessment of soil erosion in a monsoon-dominated mountain river basin in India using RUSLE-SDR and AHP. Hydrol Sci J 63:542–560. https://doi.org/10.1080/02626667.2018.1429614

Toubal AK, Achite M, Ouillon S, et al. (2018) Soil erodibility mapping using the RUSLE model to prioritize erosion control in the Wadi Sahouat basin, North-West of Algeria. Environ Monit Assess 190:210–231. https://doi.org/10.1007/s10661-018-6580-z

Tribak A, El Garouani A, Abahrour M (2012) Hydrous erosion in the catchment area of the Wadi Iarbaa (Rif Mountains, Morocco): agents, processes and modeling. Present Environ Sustain Dev 6:7–20

Tsegaye L, Bharti R (2021) Soil erosion and sediment yield assessment using RUSLE and GIS-based approach in Anjeb watershed, Northwest Ethiopia. SN Appl Sci 3:. https://doi.org/10.1007/s42452-021-04564-x

USDA-SCS (1983) National engineering handbook. Section 3, Sedimentation. U.S. Dept. of Agriculture, Soil Conservation Service, Washington, D.C., USA.

Van der Knijff J, Jones R, Montanarella L (2000) Soil erosion risk assessment in Europe. European Soil Bureau, Luxembourg, p 34.

Vanoni VA (1975) Sediment deposition engineering. ASCE Manuals and Reports on Engineering Practices, No. 54, p 745.

Wall GJ, Coote DR, Pringle EA, et al. (2002) RUSLEFAC— Revised universal soil loss equation for application in Canada: A handbook for estimating soil loss from water erosion in Canada. Res Branch, Agric Agri-Food Canada Ottawa Contrib No AAFC/AAC2244E 117.

Wischmeier WH, Smith DD (1978) Predicting rainfall erosion losses: a guide to conservation planning. Department of Agriculture, Science and Education Administration, Washington, DC, USA. p 52.

Zini A, Grauso S, Verrubbi V, et al. (2015) The RUSLE erosion index as a proxy indicator for debris flow susceptibility. Landslides 12:847–859. https://doi.org/10.1007/S10346-014-0515-8